*J. Phys. Chem. A* **2007,** *111,* 5913−5920

# Structure Enhancement Methodology Using Theory and Experiment: Gas-Phase Molecular Structures Using a Dynamic Interaction between Electron Diffraction, Molecular Mechanics, and Ab Initio Data

**Graeme R. Kafka, Sarah L. Masters,[†] and David W. H. Rankin***

*School of Chemistry, University of Edinburgh, West Mains Road, Edinburgh EH9 3JJ, United Kingdom*

*Received: April 3, 2007; In Final Form: May 1, 2007*

A new method of incorporating ab initio theoretical data dynamically into the gas-phase electron diffraction (GED) refinement process has been developed to aid the structure determination of large, sterically crowded molecules. This process involves calculating a set of differences between parameters that define the positions of peripheral atoms (usually hydrogen), as determined using molecular mechanics (MM), and those which use ab initio methods. The peripheral-atom positions are then updated continually during the GED refinement process, using MM, and the returned positions are modified using this set of differences to account for the differences between ab initio and MM methods, before being scaled back to the average parameters used to define them, as refined from experimental data. This allows the molecule to adopt a completely asymmetric structure if required, without being constrained by the MM parametrization, whereas the calculations can be performed on a practical time scale. The molecular structures of tri-*tert*-butylphosphine oxide and tri-*tert*-butylphosphine imide have been re-examined using this new technique, which we call SEMTEX (Structure Enhancement Methodology using Theory and EXperiment).

## Introduction

Gas-phase electron diffraction (GED) is effectively the only method available for determining structures of molecules that contain ∼20−100 atoms in the gas phase. GED works well, provided the molecules are symmetric; however, for structures with low symmetry, extra information is often required to make reliable structure determinations.

Initially, assumptions of local symmetry were often made to reduce the number of refining parameters. These were applied most often to light atoms. For example, a *tert*-butyl group often would be constrained to $C_3$ or $C_{3v}$ local symmetry. However, ab initio calculations have shown that such assumptions often are not valid, and the artificial constraints can have a serious and damaging influence on the resultant structure.

Accordingly, several attempts have been made to eliminate the need for such symmetry assumptions. The MOCED (Molecular Orbital Constrained Electron Diffraction)[1] and SARACEN (Structural Analysis Restrained by Ab initio Calculations for Electron diffractioN)[2−4] methods were developed with this goal. MOCED uses ab initio values to constrain small differences between certain parameters. SARACEN, on the other hand, uses computed values as flexible restraints, and this allows all parameters to be refined.

Although these methods have enabled a far greater range of molecules to be studied using GED, structural studies still frequently rely on constraints being applied to the peripheral atoms in a structure. This can significantly affect structures of sterically crowded molecules, where the outer atoms, usually hydrogen, may be displaced significantly by interactions with other atoms. Attempting to remove the symmetry constraints on the light atoms using the SARACEN method would, however, lead to a greater number of refining parameters than could be reasonably expected to refine satisfactorily to fit the electron-diffraction data.

To overcome this problem, the DYNAMITE (DYNAMic Interaction of Theory and Experiment)[5] method was recently developed. This uses rapid, low-level calculations, usually molecular mechanics (MM), linked to the refinement program to update the positions of the light atoms dynamically throughout the refinement process. This removes the need for symmetry assumptions for the peripheral atoms and allows complete asymmetry, if required.

However, MM is parametrized, and, therefore, light atoms are not completely free to find their optimal geometries. Ideally, an ab initio computational method would be used for the dynamic updating of the light-atom positions. However, computing time limitations mean that such methods cannot be implemented directly.

We have now developed the SEMTEX (Structure Enhancement Methodology for Theory and EXperiment) method to solve this problem. This method indirectly includes the results of ab initio calculations in the refinement process in the form of a calculated set of differences between these parameters and those from MM. In this way, it has been possible to incorporate high-level theoretical data into the original DYNAMITE method, while retaining computational feasibility. The differences may be recalculated once or twice during the refinements, to ensure that the final structure is effectively constrained entirely by the high-level, ab initio calculations. The results of the first two structure determinations performed using this new method are reported here.

For this work, slight improvements to the scaling routines in the DYNAMITE code have been implemented. Small scaling

---

* To whom correspondence should be addressed. E-mail: d.w.h.rankin@ed.ac.uk.

[†] Formerly Sarah L. Hinchley.

10.1021/jp072614x CCC: $37.00 © 2007 American Chemical Society
Published on Web 06/14/2007

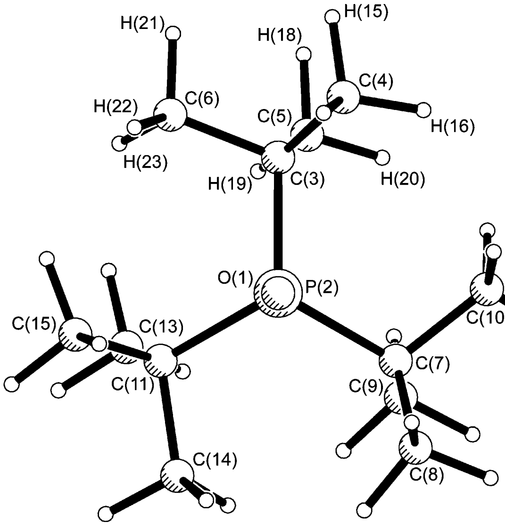

**Figure 1.** Gas-phase molecular structure of $\mathrm{OPBu}^t_3$, viewed along the O−P bond ($C_3$ rotation axis).

errors, previously undetectably small, were revealed by the wider range of values produced during the SEMTEX studies.

The structures of both tri-*tert*-butylphosphine oxide ($\mathrm{OPBu}^t_3$) and tri-*tert*-butylphosphine imide have previously been investigated using the SARACEN and DYNAMITE methods.[5,6] In this work, these refinements have been re-evaluated and the results used as starting geometries for structural analyses using the new SEMTEX method. They have been chosen so that maximum insight can be gained into the workings of the new method.

## Experimental Section

**Computational Methods.** All geometry optimizations were performed on the Columbus cluster, maintained by the National Service for Computational Chemistry Software (NSCCS),[7] using the Gaussian 03 program.[8] All second-order Møller−Plesset (MP2) calculations were frozen core [MP2(fc)]. Our implementation of the DYNAMITE optimization method uses the TINKER molecular mechanics package with the MM3 parameter set.[9]

For each of the molecules under investigation, only one conformer was located, and geometry optimizations were conducted at the RHF level, using the 6-31G* basis set,[10−12] and at the MP2 level, using the 6-311G* basis set.[13,14] The lowest energy structures are shown in Figures 1 ($\mathrm{OPBu}^t_3$) and 2 ($\mathrm{HNPBu}^t_3$). The force fields were obtained using analytic second derivatives of the energy, with respect to nuclear coordinates calculated at the RHF/6-31G* level. These were then used to provide estimates of the amplitudes of vibration for use in the GED refinements, using the SHRINK program.[15,16] The vibrational correction terms can be found in the Supporting Information. The force fields were also used to calculate the frequencies for the optimized structures. All calculated frequencies were real, indicating that each structure represented a minimum on the global potential-energy surface (PES) for that molecule.

**Electron Diffraction Data.** Original digital molecular-intensity scattering intensity data for both $\mathrm{OPBu}^t_3$ and $\mathrm{HNPBu}^t_3$[17] were reintroduced directly into the ed@ed Edinburgh electron diffraction refinement program[18] without further modification. The scattering factors of Ross et al. were used in the refinements.[19]

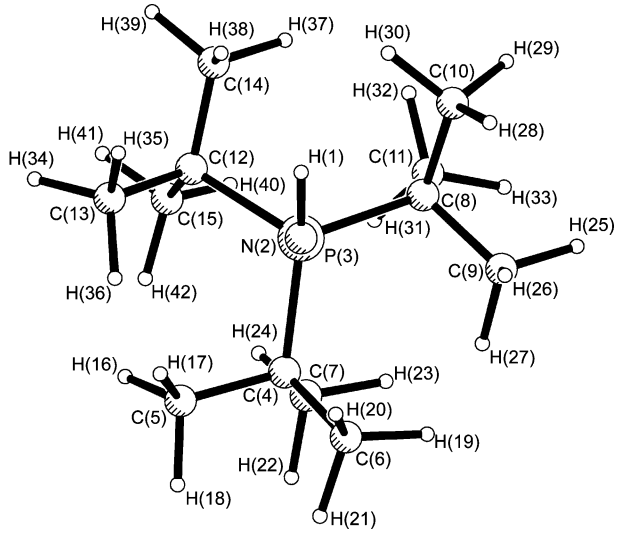

**Figure 2.** Gas-phase molecular structure of $\mathrm{HNPBu}^t_3$, viewed along the N−P bond. In this case, the molecule has $C_1$ symmetry.

**Electron Diffraction Model.** *Tri-tert-butylphosphine Oxide*. The structure was defined using a model with $C_3$ symmetry, as indicated by the ab initio calculations described previously. Fifteen independent geometric parameters were required, comprising four bond lengths, 7 bond angles and differences, and four torsion parameters. These can be found in Table 1. The starting values used for the parameters in the model were the $r_e$ values taken from the MP2 calculation; these were then applied to refine our experimental data in the ed@ed program to give the $r_{h1}$ structure.

The heavy-atom bond lengths were described by $r$(C−C), $r$(P−C), and $r$(P−O) ($p_{1-3}$). Ab initio calculations showed that, although, in principle, there are three different C−C distances in a *tert*-butyl group, the differences are insignificantly small. Experience has shown that, in such cases, refinement of all of the distances as independent parameters, restrained by computed differences, leads to the same differences and uncertainties being returned by the refinement. In such cases, this procedure is of no benefit, and we therefore fix the differences, either to the computed values or, if these are very small, to zero.

Independent heavy-atom bond-angle parameters were ∠(O−P−C) ($p_4$), an average and two difference parameters [denoted as P(2)−C(3)−C(4) minus P(2)−C(3)−C(5) and P(2)−C(3)−C(4) minus P(2)−C(3)-C(6)] to describe the P−C−C angles ($p_{5-7}$), and two C−C−C angles [C(4)−C(3)-C(5) and C(4)−C(3)-C(6)] ($p_{8,9}$). An angle that describes the torsion of the *tert*-butyl group around the P−C bond was also included ($p_{10}$).

Five parameters were also included to describe the starting positions of the H atoms. These comprised an average bond distance $r$(C−H) ($p_{11}$), an average bond angle ∠(C−C−H) ($p_{12}$), and three parameters to describe the torsions of the three methyl groups about their respective C−C bonds ($p_{13-15}$). Therefore, in the DYNAMITE and SEMTEX refinements, $p_{11}$ and $p_{12}$ represented the mean values of those for all nine H atoms in a *tert*-butyl group. The differences between values for each individual atom are set using the SEMTEX method, allowing a fully asymmetric description of the structure, as detailed below.

*Tri-tert-butylphosphine Imide.* The structure was defined using a model of $C_1$ symmetry. Altogether, 42 independent geometric parameters were required to describe the structure, comprising 7 bond lengths and differences, 22 bond angles and differences, and 13 torsion parameters. These can be found in Table 2.

The bond lengths were described by the N−H distance ($p_1$), the average and difference of the C−C and P−N bond lengths

TABLE 1: Refined and Calculated Parameters for $\mathrm{OPBu}^{t}_{3}$ from the SARACEN, DYNAMITE, and SEMTEX Studies[a]

| no. | parameter | MP2/6-311G* ($r_e$) | SARACEN ($r_{h1}$) | DYNAMITE ($r_{h1}$) | SEMTEX ($r_{h1}$) | restraint |
|---|---|---|---|---|---|---|
| $p_1$ | $r$(C−C) | 153.8 pm | 154.0(2) pm | 153.9(2) pm | 154.0(2) pm | |
| $p_2$ | $r$(C−P) | 189.0 pm | 189.1(3) pm | 189.0(2) pm | 188.7(2) pm | |
| $p_3$ | $r$(P−O) | 151.0 pm | 149.9(5) pm | 149.8(5) pm | 149.8(5) pm | 149.8(6) pm |
| $p_4$ | ∠(O−P−C) | 109.5° | 107.6(3)° | 107.6(2)° | 107.7(2)° | |
| $p_5$ | ∠(P−C−C) av. | 111.0° | 111.6(2)° | 111.6(2)° | 111.9(1)° | |
| $p_6$ | ∠(P(2)−C(3)−C(4)) − ∠(P(2)−C(3)−C(5)) | −8.4° | −9.6(8)° | −10.3(7)° | −10.7(7)° | |
| $p_7$ | ∠(P(2)−C(3)−C(4)) − ∠(P(2)−C(3)−C(6)) | −1.7° | −1.8(7)° | −1.9(7)° | −2.1(7)° | −1.7(10)° |
| $p_8$ | ∠(C(4)−C(3)−C(5)) | 109.6° | 111.9(7)° | 111.8(5)° | 111.4(7)° | |
| $p_9$ | ∠(C(4)−C(3)−C(6)) | 105.1° | 107.2(4)° | 107.2(4)° | 107.2(4)° | |
| $p_{10}$ | $\phi$(O−P−C−C(4)) | 40.5° | 36.7(8)° | 36.2(7)° | 36.2(7)° | |
| $p_{11}$ | $r$(C−H) | 109.2 pm | 108.1(2) pm | 108.0(2) pm | 108.0(2) pm | |
| $p_{12}$ | ∠(C−C−H) | 111.0° | 111.0(6)° | 111.7(4)° | 112.2(4)° | |
| $p_{13}$ | $\phi$(P−C−C(4)−H(15)) | −169.3° | −167.1(24)° | −167.4(24)° | −167.7(24)° | −168.9(26)° |
| $p_{14}$ | $\phi$(P−C−C(5)−H(18)) | 176.7° | 176.6(25)° | 176.7(27)° | 176.2(26)° | 176.6(26)° |
| $p_{15}$ | $\phi$(P−C−C(6)−H(21)) | 169.1° | 168.9(24)° | 169.4(24)° | 169.1(24)° | 169.3(27)° |

[a] Legend: $r$(X−Y), bond distance between sites X and Y; ∠(X−Y−Z), bond angle between sites X, Y, and Z; $\phi$(W−X−Y−Z), bond torsion between sites W, X, Y, and Z. The uncertainty in each measurement is given in parentheses.

TABLE 2: Refined and Calculated Parameters for $\mathrm{HNPBu}^{t}_{3}$ for the SARACEN, DYNAMITE, and SEMTEX Studies[a]

| no. | parameter | MP2/6-311G* ($r_e$) | SARACEN ($r_{h1}$) | DYNAMITE ($r_{h1}$) | SEMTEX ($r_{h1}$) | restraint |
|---|---|---|---|---|---|---|
| $p_1$ | $r$(N−H) | 101.6 pm | 101.1(5) pm | 101.1(6) pm | 101.1(5) pm | 101.0(5) pm |
| $p_2$ | $r$(C−C/P−N) av. | 154.2 pm | 155.9(2) pm | 156.0(2) pm | 155.9(2) pm | |
| $p_3$ | $r$(C−C/P−N) diff | 5.0 pm | 5.4(5) pm | 5.4(5) pm | 5.4(5) pm | 5.0(5) pm |
| $p_4$ | $r$(P−C) av. | 189.8 pm | 190.4(4) pm | 191.2(4) pm | 191.1(5) | |
| $p_5$ | $r$(P−C) d1 | −2.4 pm | −2.4(5) pm | −2.4(6) pm | −2.5(5) pm | −2.4(5) pm |
| $p_6$ | $r$(P−C) d2 | −2.5 pm | −2.7(5) pm | −2.5(6) pm | −2.5(5) pm | −2.7(5) pm |
| $p_7$ | ∠(P−C−C) av. (gp 1) | 110.9° | 110.9(8)° | 111.2(9)° | 111.1(9)° | 110.9(10)° |
| $p_8$ | ∠(P−C−C) d1 (gp 1) | 0.6° | −0.2(10)° | −0.4(10)° | −0.4(10)° | 0.6(10)° |
| $p_9$ | ∠(P−C−C) d2 (gp 1) | −6.1° | −5.5(10)° | −5.1(10)° | −5.0(10)° | −6.0(10)° |
| $p_{10}$ | ∠(C(5)−C(4)−C(6)) | 108.4° | 108.1(10)° | 107.9(11)° | 107.9(11)° | 108.4(10)° |
| $p_{11}$ | ∠(C(5)−C(4)−C(7)) | 105.5° | 105.1(10)° | 105.6(10)° | 105.7(10)° | 105.4(10)° |
| $p_{12}$ | ∠(P−C−C) av. (gp 2) | 111.1° | 112.5(10)° | 111.7(10)° | 111.6(10)° | |
| $p_{13}$ | ∠(P−C−C) d1 (gp 2) | 0.9° | 1.6(10)° | 1.1(11)° | 1.2(11)° | 0.9(10)° |
| $p_{14}$ | ∠(P−C−C) d2 (gp 2) | −8.3° | −8.3(10)° | −8.0(10)° | −8.1(10)° | −8.3(10)° |
| $p_{15}$ | ∠(C(9)−C(8)−C(10)) | 104.7° | 104.6(10)° | 104.8(11)° | 104.9(11)° | 104.7(10)° |
| $p_{16}$ | ∠(C(9)−C(8)−C(11)) | 108.5° | 108.5(10)° | 108.5(11)° | 108.6(11)° | 108.6(10)° |
| $p_{17}$ | ∠(P−C−C) av. (gp 3) | 111.2° | 109.6(11)° | 106.7(9)° | 106.5(9)° | |
| $p_{18}$ | ∠(P−C−C) d1 (gp 3) | −1.4° | −1.0(10)° | −1.5(11)° | −1.5(11)° | −1.3(10)° |
| $p_{19}$ | ∠(P−C−C )d2 (gp 3) | −8.2° | −8.4(10)° | −8.7(10)° | −8.8(10)° | −8.1(10)° |
| $p_{20}$ | ∠(C(13)−C(12)−C(14)) | 105.2° | 105.4(10)° | 106.3(10)° | 106.4(10)° | 105.2(10)° |
| $p_{21}$ | ∠(C(13)−C(12)−C(15)) | 109.1° | 109.6(10)° | 110.2(11)° | 110.3(11)° | 109.1(10)° |
| $p_{22}$ | ∠(N−P−C) av. | 106.5° | 107.3(3)° | 107.2(3)° | 107.2(3)° | |
| $p_{23}$ | ∠(N−P−C) d1 | 10.3° | 9.9(13)° | 11.8(14)° | 11.8(15)° | 10.3(15)° |
| $p_{24}$ | ∠(N−P−C) d2 | 0.8° | 0.7(15)° | −0.6(15)° | −0.5(15)° | 0.8(15)° |
| $p_{25}$ | ∠(C(4)−P(3)−C(8)) | 109.7° | 109.7(9)° | 110.5(9)° | 110.6(9)° | 109.7(10)° |
| $p_{26}$ | ∠(C(4)−P(3)−C(12)) | 109.8° | 110.1(8)° | 109.8(8)° | 109.7(8)° | 109.8(10)° |
| $p_{27}$ | ∠(P−N−H) | 115.7° | 115.8(11)° | 115.9(11)° | 115.9(11)° | 115.7(10)° |
| $p_{28}$ | $\phi$(N(2)−P(3)−C(4)−C(5)) | 73.8° | 74.3(21)° | 72.1(21)° | 72.3(20)° | 73.8(25)° |
| $p_{29}$ | $\phi$(N(2)−P(3)−C(8)−C(9)) | 67.6° | 67.2(19)° | 66.4(20)° | 66.8(21)° | 67.6(25)° |
| $p_{30}$ | $\phi$(N(2)−P(3)−C(12)−C(13)) | −36.3° | −34.7(20)° | −39.3(21)° | −39.6(20)° | −36.3(25)° |
| $p_{31}$ | $\phi$(H−N−P−C) | −173.0° | −173.0(11)° | −173.0(11)° | −173.0(11)° | −172.9(10)° |
| $p_{32}$ | $r$(C−H) | 109.2 pm | 114.5(3) pm | 114.9(3) pm | 115.0(3) pm | |
| $p_{33}$ | ∠(C−C−H) | 107.6° | 108.6(8)° | 110.4(7)° | 110.5(8)° | |
| $p_{34}$ | $\phi$(P(3)−C(4)−C(5)−H(16)) | 72.6° | 70.9(26)° | 71.4(27)° | 71.4(27)° | 72.6(25)° |
| $p_{35}$ | $\phi$(P(3)−C(4)−C(6)−H(19)) | −70.3° | 176.4(27)° | 176.3(27)° | 176.5(27)° | 175.9(25)° |
| $p_{36}$ | $\phi$(P(3)−C(4)−C(7)−H(22)) | −175.9° | 69.4(26)° | 69.4(27)° | 69.7(27)° | 70.2(25)° |
| $p_{37}$ | $\phi$(P(3)−C(8)−C(9)−H(25)) | 73.8° | 73.1(26)° | 73.5(28)° | 73.7(28)° | 73.8(25)° |
| $p_{38}$ | $\phi$(P(3)−C(8)−C(10)−H(28)) | 54.9° | 67.3(26)° | 67.4(27)° | 68.1(27)° | 68.0(25)° |
| $p_{39}$ | $\phi$(P(3)−C(8)−C(11)−H(31)) | 66.2° | 175.3(27)° | 175.3(27)° | 175.4(27)° | 175.4(25)° |
| $p_{40}$ | $\phi$(P(3)−C(12)−C(13)−H(34)) | −71.1° | 50.4(27)° | 50.0(27)° | 50.1(27)° | 50.6(25)° |
| $p_{41}$ | $\phi$(P(3)−C(12)−C(14)−H(37)) | −51.9° | 53.3(26)° | 52.5(27)° | 52.8(27)° | 51.9(25)° |
| $p_{42}$ | $\phi$(P(3)−C(12)−C(15)−H(40)) | −57.3° | 177.4(26)° | 176.3(27)° | 177.1(27)° | 176.2(25)° |

[a] Legend: $r$(X−Y), bond distance between sites X and Y; ∠(X−Y−Z), bond angle between sites X, Y, and Z; $\phi$(W−X−Y−Z), bond torsion between sites W, X, Y, and Z. The uncertainty in each measurement is given in parentheses.

($p_{2-3}$), and the average and two differences for the P−C bond lengths ($p_{4-6}$). Independent bond-angle parameters included three average and difference parameters for the P−C−C angles of each *tert*-butyl group ($p_{7-9,12-14,17-19}$), with two associated C−C−C angles ($p_{10,11,15,16,20,21}$). The P−N−H angle was also used ($p_{27}$), as were two C−P−C angles ($p_{25,26}$), and average and two difference parameters to describe the N−P−C angles ($p_{22-24}$). Torsional parameters were three *tert*-butyl group

**TABLE 3: C−H Bond Lengths, C−C−H Bond Angles, and P−C−C−H Bond Torsions for OPBu$^{t}_{3}$, Calculated with the MM3 and MP2/6-311G* Methods[a]**

| parameter | *r*(C−H) (pm) |  | ∠(C−C−H) (deg) |  | *ϕ*(P−C−C−H) (deg) |  |
|---|---|---|---|---|---|---|
|  | MM3 | MP2 | MM3 | MP2 | MM3 | MP2 |
| P(2)−C(3)−C(4)−H(15) | 111.3 | 109.6 | 111.1 | 108.2 | −173.6 | −168.5 |
| P(2)−C(3)−C(4)−H(16) | 110.7 | 108.9 | 113.1 | 113.0 | 67.3 | 72.5 |
| P(2)−C(3)−C(4)−H(17) | 111.1 | 109.1 | 112.3 | 110.4 | −54.5 | −49.3 |
| P(2)−C(3)−C(5)−H(18) | 111.3 | 109.5 | 111.9 | 108.4 | 173.8 | 175.7 |
| P(2)−C(3)−C(5)−H(19) | 111.1 | 109.3 | 111.7 | 111.5 | 53.7 | 57.5 |
| P(2)−C(3)−C(5)−H(20) | 110.7 | 109.1 | 113.0 | 114.0 | −66.7 | −65.1 |
| P(2)−C(3)−C(6)−H(21) | 111.3 | 109.5 | 111.5 | 107.9 | 173.8 | 173.4 |
| P(2)−C(3)−C(6)−H(22) | 111.1 | 109.3 | 111.1 | 111.9 | 56.0 | 55.8 |
| P(2)−C(3)−C(6)−H(23) | 110.6 | 108.8 | 113.8 | 113.1 | −66.4 | −67.7 |
| range | 0.7 | 0.8 | 2.7 | 6.1 | N/A | N/A |

[a] Internuclear distances are the calculated ($r_e$) values.

**TABLE 4: C−H Bond Lengths, C−C−H Bond Angles, and P−C−C−H Bond Torsions for OPBu$^{t}_{3}$ for Both the DYNAMITE and SEMTEX Refinements**

| parameter | Bond Length, *r*(C−H) ($r_{h1}$) (pm) |  | Bond Angle, ∠(C−C−H) (deg) |  | Bond Torsion, *ϕ*(P−C−C−H) (deg) |  |
|---|---|---|---|---|---|---|
|  | DYNAMITE | SEMTEX | DYNAMITE | SEMTEX | DYNAMITE | SEMTEX |
| P(2)−C(3)−C(4)−H(15) | 108.2 | 108.0 | 110.6 | 109.6 | −167.5 | −167.6 |
| P(2)−C(3)−C(4)−H(16) | 107.6 | 107.2 | 112.5 | 114.2 | 73.5 | 73.4 |
| P(2)−C(3)−C(4)−H(17) | 108.1 | 107.5 | 111.8 | 111.7 | −48.3 | −48.6 |
| P(2)−C(3)−C(5)−H(18) | 108.2 | 107.9 | 111.5 | 109.9 | 174.8 | −178.8 |
| P(2)−C(3)−C(5)−H(19) | 108.1 | 107.7 | 112.4 | 112.8 | 54.6 | 61.4 |
| P(2)−C(3)−C(5)−H(20) | 107.6 | 107.5 | 111.1 | 115.4 | −65.7 | −59.0 |
| P(2)−C(3)−C(6)−H(21) | 108.2 | 107.9 | 111.1 | 109.3 | 168.6 | 169.3 |
| P(2)−C(3)−C(6)−H(22) | 108.1 | 107.8 | 110.6 | 113.2 | 50.0 | 51.3 |
| P(2)−C(3)−C(6)−H(23) | 107.5 | 107.2 | 113.3 | 114.4 | −71.4 | −71.3 |
| range | 0.7 | 0.8 | 2.7 | 6.1 | N/A | N/A |

torsions [*ϕ*(N(2)−P(3)−C(4)−C(5)), *ϕ*(N(2)−P(3)−C(8)−C(9)), and *ϕ*(N(2)−P(3)-C(12)−C(13))] ($p_{28-30}$), and *ϕ*(H−N−P−C(4)) ($p_{31}$).

Finally, 11 parameters were included to describe the starting positions of the peripheral H atoms. These comprised the mean C−H bond length ($p_{32}$), the mean ∠(C−C−H) bond angle ($p_{33}$), and 9 parameters to describe the torsions of the three methyl groups in each butyl group about their adjacent C−C bonds ($p_{34-42}$). Again, in the DYNAMITE and SEMTEX refinements, $p_{32}$ and $p_{33}$ represented the mean values of those for all nine H atoms in a *tert*-butyl group.

*SEMTEX Methodology*. Initially, the heavy-atom structure of the molecule is determined via a standard SARACEN GED refinement (i.e., (flexibly) restrained where necessary by parameters calculated ab initio). The Cartesian coordinates of this refined structure are output to a data file. Geometry optimizations at both the ab initio and MM levels of theory are then performed, with the heavy-atom coordinates fixed to their refined GED values in each case. These optimizations are, of course, constrained, and do not lead to the absolutely lowest-energy structures for the molecule. However, the procedure does yield the potential minima for the constrained structure at the two levels of theory, and should therefore give the best representation of the H-atom positions in the real molecule. The procedure gives two sets of light-atom coordinates, whose differences are attributable entirely to the effects of the differing levels of theory used. The position of each H atom in each computed structure is then derived in terms of a C−H bond length, C−C−H angle, and P−C−C−H dihedral angle. By subtracting the MP2 values of these three parameters from the MM-determined values, a set of difference parameters is obtained. These are then introduced as additional data in the refinement process, modifying the parameters that are returned continually by the MM code to reflect the differences between the two levels of theory. Thus, the absolute differences between H-atom parameters are derived ab initio, but they are modified dynamically at the MM level. Thus, the average distance, average angle, and three torsional parameters that describe the H-atom positions are still refined from the experimental data, with the differences between the absolute values for the individual atoms being effectively calculated ab initio.

Because of the fact that the entire structure refines using this method, the initial heavy-atom structure (as calculated by the SARACEN method) will change over several cycles of refinement. This renders the initial set of differences obsolete, because they were calculated based on heavy-atom coordinates frozen at values that are no longer valid. As a consequence, it is necessary to repeat the theoretical calculations periodically and recalculate the difference set during the refinement. The method works with any two types of calculations, such as an expensive, high-level calculation that is performed few times, and a low-level, inexpensive calculation that is performed repeatedly.

## Results

**Tri-*tert*-butylphosphine Oxide.** *Theoretical Methods*. The structure of OPBu$^{t}_{3}$ was determined ab initio. A previous PES search[5] involving rotation of the *tert*-butyl groups around the P−C bonds found only one conformer of OPBu$^{t}_{3}$, which exhibited $C_3$ symmetry. GED refinements can be complicated by the presence of multiple conformers, which we therefore wish to avoid at this stage. Thus, the presence of only one conformer makes this molecule well-suited to be a test case for the new method. The molecular geometry of OPBu$^{t}_{3}$ at the MP2/6-311G* level can be found in Table 1.

At the outset of the SEMTEX refinement process, the heavy-atom positions were fixed as calculated using DYNAMITE, and both MP2/6-311G* and MM3 calculations were performed on

**TABLE 5: C−H Bond Lengths, C−C−H Bond Angles, and P−C−C−H Bond Torsions for HNPBu$^t_3$ Calculated with the MM3 and MP2/6-311G* Methods**[a]

| parameter | Bond Length, $r$(C−H) (pm) | | Bond Angle, ∠(C−C−H) (deg) | | Bond Torsion, $\phi$(P−C−C−H) (deg) | |
|---|---|---|---|---|---|---|
| | MM3 | MP2 | MM3 | MP2 | MM3 | MP2 |
| P(3)−C(4)−C(5)−H(16) | 110.8 | 108.8 | 112.8 | 113.7 | 76.1 | 74.5 |
| P(3)−C(4)−C(5)−H(17) | 111.2 | 108.9 | 113.4 | 111.2 | −49.9 | −50.7 |
| P(3)−C(4)−C(5)−H(18) | 111.3 | 109.6 | 110.8 | 107.7 | −168.0 | −168.5 |
| P(3)−C(4)−C(6)−H(19) | 110.7 | 108.9 | 113.4 | 113.8 | −63.8 | −64.2 |
| P(3)−C(4)−C(6)−H(20) | 111.3 | 109.1 | 112.4 | 110.0 | 57.5 | 57.1 |
| P(3)−C(4)−C(6)−H(21) | 111.3 | 109.5 | 111.8 | 107.7 | 177.2 | 176.5 |
| P(3)−C(4)-C(7)−H(22) | 111.3 | 109.8 | 110.7 | 109.1 | −171.6 | −171.4 |
| P(3)−C(4)−C(7)−H(23) | 110.8 | 109.1 | 113.0 | 111.8 | 70.3 | 70.8 |
| P(3)−C(4)−C(7)−H(24) | 110.6 | 108.8 | 114.3 | 113.9 | −52.2 | −51.9 |
| P(3)−C(8)−C(9)−H(25) | 110.8 | 109.0 | 113.1 | 113.2 | 72.4 | 73.3 |
| P(3)−C(8)−C(9)−H(26) | 111.3 | 109.6 | 111.3 | 108.0 | −169.4 | −168.1 |
| P(3)−C(8)−C(9)−H(27) | 111.2 | 109.3 | 112.5 | 111.1 | −50.7 | −49.8 |
| P(3)−C(8)−C(10)−H(28) | 111.2 | 109.3 | 112.6 | 110.9 | 55.3 | 55.2 |
| P(3)−C(8)−C(10)−H(29) | 111.3 | 109.5 | 111.6 | 108.3 | 174.6 | 173.4 |
| P(3)−C(8)−C(10)−H(30) | 110.8 | 109.0 | 113.3 | 113.6 | −66.4 | −67.4 |
| P(3)−C(8)−C(11)−H(31) | 111.1 | 109.4 | 112.0 | 112.0 | 61.9 | 62.5 |
| P(3)−C(8)−C(11)−H(32) | 111.3 | 109.6 | 111.8 | 108.9 | −178.6 | −178.9 |
| P(3)−C(8)−C(11)−H(33) | 111.0 | 109.3 | 112.4 | 112.7 | −58.7 | −59.7 |
| P(3)−C(12)−C(13)−H(34) | 110.5 | 108.3 | 114.9 | 113.6 | −87.3 | −89.9 |
| P(3)−C(12)−C(13)−H(35) | 111.3 | 109.6 | 109.4 | 107.8 | 157.3 | 152.9 |
| P(3)−C(12)−C(13)−H(36) | 111.1 | 109.9 | 115.2 | 112.2 | 39.9 | 34.7 |
| P(3)−C(12)−C(14)−H(37) | 111.2 | 109.2 | 113.9 | 110.6 | −49.2 | −49.9 |
| P(3)−C(12)−C(14)−H(38) | 111.3 | 109.7 | 110.7 | 109.1 | −169.0 | −168.0 |
| P(3)−C(12)−C(14)−H(39) | 111.0 | 109.2 | 111.7 | 113.0 | 74.1 | 72.8 |
| P(3)−C(12)−C(15)−H(40) | 111.0 | 109.3 | 112.4 | 113.1 | −56.1 | −57.3 |
| P(3)−C(12)−C(15)−H(41) | 111.3 | 109.9 | 110.0 | 109.5 | −174.0 | −177.0 |
| P(3)−C(12)−C(15)−H(42) | 110.8 | 108.7 | 113.9 | 110.7 | 67.6 | 65.2 |
| range | 0.8 | 1.6 | 5.8 | 6.2 | N/A | N/A |

[a] Internuclear distances are the calculated ($r_e$) values.

the light atoms. The resulting light-atom parameters can be found in Table 3. As the values in Table 3 show, the C−C−H angles at the MP2 level of theory cover a range of 6.1°, whereas for the MM3 calculation, this variation is much smaller (∼2.7°). Clearly, this is a significant difference in the structure as determined by these different theoretical methods. The inclusion of the ab initio data in the refinement via the SEMTEX method will allow this and other structural features to be modeled more accurately. (The values of the C−H bond lengths, C−C−H bond angles, and P−C−C−H bond torsions for OPBu$^t_3$, using the DYNAMITE and SEMTEX methods, can be found in Table 4.)

*SARACEN GED Refinement*. The starting parameters for the $r_{h1}$ refinement were taken from the theoretical geometry optimized at the MP2/6-311G* level. Fifteen geometric parameters were refined, along with 21 groups of vibrational amplitudes. Five geometric and nine amplitude restraints were applied according to the SARACEN method; these can be found in Table 1. The final $R$ factors for the refinement were determined to be $R_G = 0.061$ and $R_D = 0.089$. Interatomic distances and corresponding amplitudes of vibration are given in Table S1 in the Supporting Information, and final experimental coordinates from the SARACEN GED analysis are given in Table S2 in the Supporting Information. The correlation matrix is given in Table S3 in the Supporting Information.

*DYNAMITE GED Refinement*. The starting parameters and force field were as described for the SARACEN refinement, and all geometric parameters were refined according to this method. After this step was complete, the DYNAMITE code was activated and the light-atom positions were updated computationally. Consequently, the parameters associated with the H atoms now represent average values over all atoms in a *tert*-butyl group. In regard to the SARACEN refinement, 15 geometric parameters and 21 groups of vibrational amplitudes were refined. The final $R$ factors for the refinement were determined to be $R_G = 0.061$ and $R_D = 0.087$. Interatomic distances and corresponding amplitudes of vibration can be found in Table S4 in the Supporting Information, and final experimental coordinates from the DYNAMITE GED analysis are given in Table S5 in the Supporting Information. The correlation matrix can be found in Table S6 in the Supporting Information.

*SEMTEX GED Refinement*. The starting parameters were as described for the SARACEN and DYNAMITE refinements. The geometric parameters were refined using, first, the SARACEN method and, then, the DYNAMITE method. After all 15 geometric parameters and 21 groups of vibrational amplitudes were refined according to the DYNAMITE method, the SEMTEX code was activated. The heavy-atom positions were fixed and theoretical structures were calculated at both the MP2 and MM3 levels of theory. The differences in the light-atom parameters between these two structures were then calculated. During each refinement cycle for each parameter, the light-atom positions returned by the MM3 code were immediately modified by this set of differences.

In regard to the SARACEN and DYNAMITE refinements, all 15 geometric parameters were refined, along with 21 groups of vibrational amplitudes. Five geometric and nine amplitude restraints were applied using the SARACEN method. In the final refinement, the $R$ factors were $R_G = 0.062$ and $R_D = 0.086$. Figure 3 shows the radial distribution curve, and Table 1 lists the final refined parameters. Interatomic distances and corresponding amplitudes of vibration are given in Table S7 in the Supporting Information and final experimental coordinates from the SEMTEX GED analysis are given in Table S8 in the Supporting Information. The correlation matrix is given in Table S9 in the Supporting Information.

**Tri-*tert*-butylphosphine Imide.** *Theoretical Methods.* The structure of HNPBu$^t_3$ was determined using both ab initio and

**TABLE 6: C−H Bond Lengths, C−C−H Bond Angles, and P−C−C−H Bond Torsions for HNPBu$^{t}_{3}$ for Both the DYNAMITE and SEMTEX Refinements**[a]

| | Bond Length, $r$(C−H) ($r_{h1}$) (pm) | | Bond Angle, ∠(C−C−H) (deg) | | Bond Torsion, $\phi$(P−C−C−H) (deg) | |
|---|---|---|---|---|---|---|
| parameter | DYNAMITE | SEMTEX | DYNAMITE | SEMTEX | DYNAMITE | SEMTEX |
| P(3)−C(4)−C(5)−H(16) | 114.6 | 114.6 | 110.8 | 113.2 | 74.7 | 74.8 |
| P(3)−C(4)−C(5)−H(17) | 115.0 | 114.7 | 111.3 | 110.7 | −51.1 | −51.2 |
| P(3)−C(4)−C(5)−H(18) | 115.2 | 115.4 | 108.9 | 107.0 | −169.3 | −169.3 |
| P(3)−C(4)−C(6)−H(19) | 114.6 | 114.7 | 111.3 | 113.2 | −70.2 | −70.5 |
| P(3)−C(4)−C(6)−H(20) | 115.1 | 114.9 | 110.4 | 109.5 | 51.1 | 50.8 |
| P(3)−C(4)−C(6)−H(21) | 115.2 | 115.3 | 109.8 | 107.3 | 170.8 | 170.5 |
| P(3)−C(4)−C(7)−H(22) | 115.2 | 115.6 | 108.8 | 108.7 | −176.7 | −176.9 |
| P(3)−C(4)−C(7)−H(23) | 114.7 | 114.9 | 111.0 | 111.3 | 65.2 | 64.9 |
| P(3)−C(4)−C(7)−H(24) | 114.5 | 114.6 | 112.2 | 113.3 | −57.3 | −57.6 |
| P(3)−C(8)−C(9)−H(25) | 114.7 | 114.8 | 111.1 | 112.7 | −177.8 | −178.0 |
| P(3)−C(8)−C(9)−H(26) | 115.2 | 115.4 | 109.4 | 107.5 | −59.7 | −59.8 |
| P(3)−C(8)−C(9)−H(27) | 115.1 | 115.0 | 110.5 | 110.6 | 59.1 | 58.9 |
| P(3)−C(8)−C(10)−H(28) | 115.1 | 115.1 | 110.6 | 110.5 | 83.1 | 83.0 |
| P(3)−C(8)−C(10)−H(29) | 115.2 | 115.3 | 109.6 | 107.9 | −157.6 | −157.7 |
| P(3)−C(8)−C(10)−H(30) | 114.7 | 114.8 | 111.3 | 113.0 | −38.5 | −38.6 |
| P(3)−C(8)−C(11)−H(31) | 115.0 | 115.2 | 110.0 | 111.5 | −29.6 | −29.4 |
| P(3)−C(8)−C(11)−H(32) | 115.1 | 115.4 | 109.8 | 108.4 | 89.9 | 90.1 |
| P(3)−C(8)−C(11)−H(33) | 114.9 | 115.1 | 110.4 | 112.1 | −150.2 | −150.1 |
| P(3)−C(12)−C(13)−H(34) | 114.3 | 114.1 | 112.8 | 113.1 | −165.9 | −165.8 |
| P(3)−C(12)−C(13)−H(35) | 115.2 | 115.7 | 107.5 | 107.3 | 78.7 | 78.9 |
| P(3)−C(12)−C(13)−H(36) | 114.9 | 114.8 | 113.2 | 111.7 | −38.9 | −38.6 |
| P(3)−C(12)−C(14)−H(37) | 115.1 | 115.0 | 111.8 | 110.1 | 60.1 | 58.9 |
| P(3)−C(12)−C(14)−H(38) | 115.1 | 115.5 | 108.8 | 108.6 | −59.7 | −60.8 |
| P(3)−C(12)−C(14)−H(39) | 114.9 | 115.0 | 109.6 | 112.5 | −176.6 | −177.7 |
| P(3)−C(12)−C(15)−H(40) | 114.9 | 115.0 | 110.4 | 112.6 | −59.9 | −60.4 |
| P(3)−C(12)−C(15)−H(41) | 115.1 | 115.7 | 108.1 | 109.1 | −177.8 | −178.3 |
| P(3)−C(12)−C(15)−H(42) | 114.7 | 114.4 | 111.8 | 110.3 | 63.7 | 63.2 |
| range | 0.9 | 1.6 | 5.7 | 6.3 | N/A | N/A |

[a] Internuclear distances are the calculated ($r_e$) values.

MM methods. In this case, only one conformer, which exhibited $C_1$ symmetry, was observed. As a consequence of the low symmetry of this molecule, the SEMTEX refinement process was considerably more time-consuming than for the OPBu$^{t}_{3}$ investigation. The molecular geometry of HNPBu$^{t}_{3}$ at the MP2/6-311G* level is given in Table 2. The values of the C−H bond lengths, C−C−H bond angles, and P−C−C−H bond torsion parameters from the MP2/6-311G* calculation are given in Table 5. As these values show, the C−C−H angles at the MP2 level of theory show a variation of 6.2°, whereas, for the MM3 calculation, this variation is 5.8°. This discrepancy between the MP2 and MM3 level calculations is less pronounced than for the OPBu$^{t}_{3}$ case.

*SARACEN GED Refinement.* The starting parameters for the $r_{h1}$ refinement were taken from the theoretical geometry optimized at the MP2/6-311G* level. In total, 42 geometric parameters were refined, along with 10 groups of vibrational amplitudes. Thirty-five geometric and six amplitude restraints were applied, according to the SARACEN method. These are given in Table S3 in the Supporting Information. The final $R$ factors for the refinement were determined to be $R_G = 0.072$ ($R_D = 0.097$). Final refined parameters are given in Table 2. Interatomic distances and corresponding amplitudes of vibration are given in Table S10 in the Supporting Information, with final experimental coordinates from the SARACEN GED analysis given in Table S11 in the Supporting Information. The correlation matrix for the refinement can be found in Table S12 in the Supporting Information.

*DYNAMITE GED Refinement.* The starting parameters and force field were as described for the SARACEN refinement, and all geometric parameters were refined according to this method. After this step was complete, the DYNAMITE code was activated and the light-atom positions were updated computationally. Consequently, the parameters associated with the H atoms now represent average values over all nine atoms in a *tert*-butyl group. As described for the SARACEN refinement, 42 geometric parameters and 10 groups of vibrational amplitudes were refined. The final $R$ factors for the refinement were determined to be $R_G = 0.068$ ($R_D = 0.097$). Final refined parameters are listed in Table 2. Interatomic distances and corresponding amplitudes of vibration can be found in Table S13 in the Supporting Information, with the final experimental coordinates from the DYNAMITE GED analysis given in Table S14 in the Supporting Information, and the correlation matrix in Table S15 in the Supporting Information.

*SEMTEX GED Refinement.* The starting parameters were as described for the SARACEN and DYNAMITE refinements. The geometric parameters were refined using, first, the SARACEN and, then, the DYNAMITE method. As for the OPBu$^{t}_{3}$ case, the SEMTEX code was then activated. In regard to the SARACEN and DYNAMITE refinements, all 42 geometric parameters were refined, along with 10 groups of vibrational amplitudes. Five geometric and nine amplitude restraints were applied, using the SARACEN method. In the final refinement, the $R$ factors were $R_G = 0.068$ ($R_D = 0.097$). Figure 4 shows the final radial distribution curve from the refinement, and Table 2 lists the final refined parameters. Interatomic distances and corresponding amplitudes of vibration are given in Table S16 in the Supporting Information, and final experimental coordinates from the SEMTEX refinement are given in Table S17 in the Supporting Information. The correlation matrix is shown in Table S18 in the Supporting Information.

As for the OPBu$^{t}_{3}$ study, no great difference is observed between the values of the refined parameters or $R$-factors for the DYNAMITE and SEMTEX refinements. This is an expected result, because both the structures involved in this study are

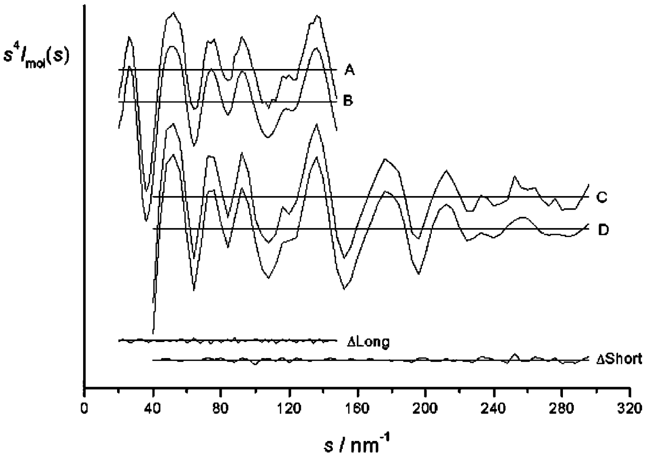

**Figure 3.** Molecular scattering intensity curves for OPBu$^{t}_{3}$. The experimental and theoretical curves are given for both the long (A and B) and short (C and D) camera distances, along with the two difference curves (ΔLong and ΔShort).

relatively simple cases, which were already well-determined using previous methods. It is expected that the new method will give reliable refinements of more-complex structures than would be possible using either the DYNAMITE or SARACEN approaches.

## Discussion

The molecular structures of tri-*tert*-butylphosphine oxide and tri-*tert*-butylphosphine imide have been re-examined as test cases for a new method of GED structure refinement that has been developed. Previously, these molecules had been studied using the DYNAMITE total structure determination method, which uses the MM method to model the positions of the H atoms throughout the refinement process.

The new SEMTEX method goes one step further by using high-level theoretical data—in this case, at the MP2 level—repeatedly within the GED refinement process. This allows a more-accurate fitting to our experimental data, effectively improving the DYNAMITE method by allowing it to make use of more-expensive computational methods than were previously possible. In the case of OPBu$^{t}_{3}$, large discrepancies were observed between the MM and ab initio calculated structures. A particularly notable example of this was the range of C—C—H angles, which was more than twice as large for the MP2 case as for the MM3 case: 6.1°, compared to 2.7°.

For the SEMTEX refinement of OPBu$^{t}_{3}$, experimental and theoretical parameters are generally in good agreement with each other. The C—C interatomic distance refined to a value of 154.0 pm, compared to a value of 153.8 pm, which was calculated at the MP2/6-311G* level of theory. Angles also were generally in agreement, to within 1.5°. For example, $\angle$(O—P—C) refined to a value of 107.7°, compared to a value of 109.1° from the calculations.

There is a very good level of agreement between the DYNAMITE and SEMTEX refinements, as was expected in this case, because of the relatively simple nature of the molecule under investigation. For the heavy atoms, the interatomic distance parameters agree to within 0.5 pm. The largest heavy-atom discrepancy occurs in the P—C interatomic distance, showing a difference of only 0.3 pm. Angles given for the two methods also are in close agreement.

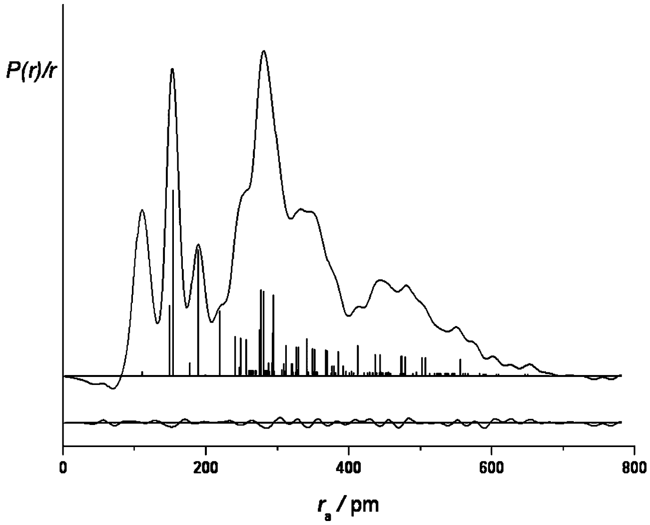

**Figure 4.** Experimental and difference (experimental − theoretical) radial distribution curves ($P(r)/r$), from the SEMTEX refinement of OPBu$^{t}_{3}$. Before Fourier inversion, the data were multiplied by a factor of $s\ \exp(-0.00002s^2)/[(Z_C - f_C)(Z_P - f_P)]$.

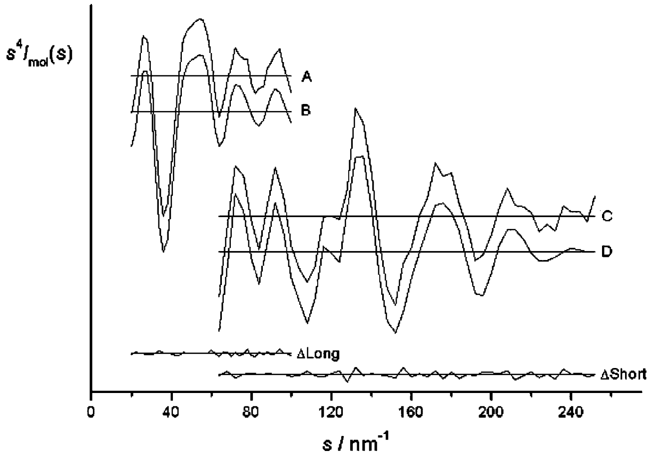

**Figure 5.** Molecular scattering intensity curves for HNPBu$^{t}_{3}$. The experimental and theoretical curves are given for both the long (A and B) and short (C and D) camera distances, along with the two difference curves (ΔLong and ΔShort).

The average light-atom parameters (C—C distance, C—C—H angle, and P—C—C—H torsion parameters, averaged over nine H atoms in a *tert*-butyl group) also agree well. However, a notable difference between the structures of the DYNAMITE and SEMTEX refinements is the range of different values for these parameters. For the DYNAMITE refinement, the range of C—C—H angles was determined to be 2.7°, whereas for the SEMTEX refinement, it was more than double this value (6.1°). This reflects the difference between the ab initio and MM structures mentioned previously, and it shows that the MM3 method used previously did not allow for the complete asymmetry that the structure should adopt.

For HNPBu$^{t}_{3}$, the range of C—C—H angles was determined to be 6.2° for the MP2 calculation and 5.8° for the MM3 calculation. This is clearly much less of a difference in ranges, when compared to the OPBu$^{t}_{3}$ structure. In this case, less difference would therefore be expected in the structures of the DYNAMITE and SEMTEX refinements. This prediction is borne out in the final refined structures, where a range of 6.3° is found for the SEMTEX refinement, in comparison with a range of 5.7° for DYNAMITE. (See Table 6 and Figures 5 and 6.)

As in the OPBu$^{t}_{3}$ case, there is very close agreement of parameters given by the DYNAMITE and SEMTEX methods.

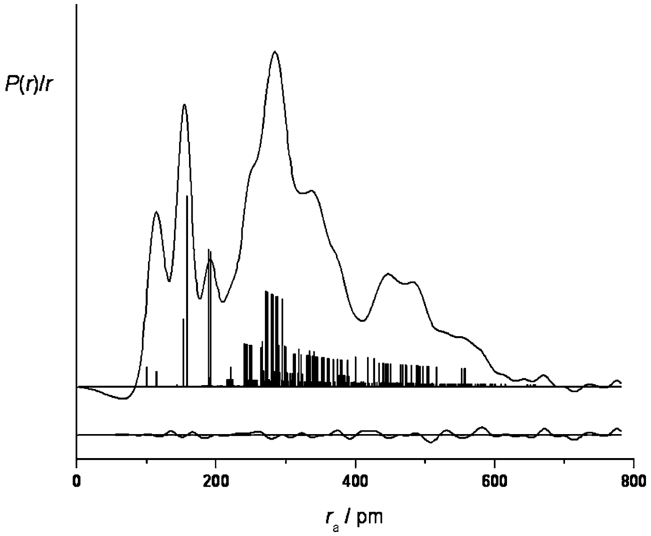

**Figure 6.** Experimental and difference (experimental − theoretical) radial distribution curves ($P(r)/r$), from the SEMTEX refinement of $HNPBu^t_3$. Before Fourier inversion, the data were multiplied by a factor of $s\ \exp(-0.00002s^2)/[(Z_C - f_C)(Z_P - f_P)]$.

The interatomic distances all agree to within 0.3 pm, with the average C−H distance are increased by this amount. Experimental and theoretical parameters are also in very good agreement. For example, the average N−P−C angle is determined to be 106.5° from ab initio calculations and 107.2° by SEMTEX methods. The light-atom parameters also agree well, with, for example, a variation of 0.3 pm in the average C−H distance between DYNAMITE and SEMTEX.

## Conclusion

The structures of two sterically crowded molecules, $OPBu^t_3$ and $HNPBu^t_3$, have been re-determined as test cases for the new SEMTEX method of total structure determination. As expected, the fit to experimental data changed little between the DYNAMITE and SEMTEX refinements for these relatively simple cases. However, the structures have finally been allowed to adopt the completely asymmetric conformations, which are shown by ab initio theoretical methods to be desirable. This new method is expected to be of primary importance in studying the structures of large, sterically crowded molecules, especially those containing significant intramolecular forces. It can be applied equally well to molecules with non-hydrogen peripheral atoms, such as metal carbonyls and fluorocarbons, where the consequences of inaccurate atom placements could be severe.

**Acknowledgment.** We thank the National Service for Computational Chemistry Software (NSCCS; http://www.nsccs.ac.uk) for computing time. Author G.R.K. thanks the University of Edinburgh for funding.

**Supporting Information Available:** Tables giving the interatomic distances ($r_a$, given in picometers) and amplitudes of vibration ($u$, given in picometers) from the SARACEN, DYNAMITE, and SEMTEX gas-phase electron diffraction (GED) refinements of the structure of $OPBu^t_3$; experimental GED coordinates from the SARACEN, DYNAMITE, and SEMTEX refinements of $OPBu^t_3$; interatomic distances ($r_a$, given in picometers) and amplitudes of vibration ($u$, given in picometers) from the SARACEN, DYNAMITE, and SEMTEX GED refinements of the structure of $HNPBu^t_3$; final GED coordinates from the SARACEN, DYNAMITE, and SEMTEX refinements of $HNPBu^t_3$. (PDF.) This material is available free of charge via the Internet at http://pubs.acs.org.

## References and Notes

(1) Chiu, N. S.; Sellers, H. L.; Schaefer, L.; Kohata, K. *J. Am. Chem. Soc.* **1979**, *101*, 5883.

(2) Brain, P. T.; Morrison, C. A.; Parsons, S.; Rankin, D. W. H. *J. Chem. Soc., Dalton Trans.* **1996**, 4589.

(3) Blake, A. J.; Brain, P. T.; McNab, H.; Miller, J.; Morrison, C. A.; Parsons, S.; Rankin, D. W. H.; Robertson, H. E.; Smart, B. A. *J. Phys. Chem.* **1996**, *100*, 12280.

(4) Mitzel, N. W.; Rankin, D. W. H. *Dalton Trans.* **2003**, 3650.

(5) Hinchley, S. L.; Haddow, M. F.; Rankin, D. W. H. *Dalton Trans.* **2004**, 384.

(6) Hinchley, S. L.; Haddow, M. F.; Rankin, D. W. H. *Inorg. Chem.* **2004**, *43*, 5522.

(7) EPSRC National Service for Computational Chemistry Software; URL: http://www.nsccs.ac.uk.

(8) Frisch, M. J.; Trucks, G. W.; Schlegel, H. B.; Scuseria, G. E.; Robb, M. A.; Cheeseman, J. R.; Montgomery, J. A., Jr.; Vreven, T.; Kudin, K. N.; Burant, J. C.; Millam, J. M.; Iyengar, S. S.; Tomasi, J.; Barone, V.; Mennucci, B.; Cossi, M.; Scalmani, G.; Rega, N.; Petersson, G. A.; Nakatsuji, H.; Hada, M.; Ehara, M.; Toyota, K.; Fukuda, R.; Hasegawa, J.; Ishida, M.; Nakajima, T.; Honda, Y.; Kitao, O.; Nakai, H.; Klene, M.; Li, X.; Knox, J. E.; Hratchian, H. P.; Cross, J. B.; Bakken, V.; Adamo, C.; Jaramillo, J.; Gomperts, R.; Stratmann, R. E.; Yazyev, O.; Austin, A. J.; Cammi, R.; Pomelli, C.; Ochterski, J. W.; Ayala, P. Y.; Morokuma, K.; Voth, G. A.; Salvador, P.; Dannenberg, J. J.; Zakrzewski, V. G.; Dapprich, S.; Daniels, A. D.; Strain, M. C.; Farkas, O.; Malick, D. K.; Rabuck, A. D.; Raghavachari, K.; Foresman, J. B.; Ortiz, J. V.; Cui, Q.; Baboul, A. G.; Clifford, S.; Cioslowski, J.; Stefanov, B. B.; Liu, G.; Liashenko, A.; Piskorz, P.; Komaromi, I.; Martin, R. L.; Fox, D. J.; Keith, T.; Al-Laham, M. A.; Peng, C. Y.; Nanayakkara, A.; Challacombe, M.; Gill, P. M. W.; Johnson, B.; Chen, W.; Wong, M. W.; Gonzalez, C.; Pople, J. A. *Gaussian 03*, revision C.01; Gaussian, Inc.: Wallingford, CT, 2004.

(9) Ponder, J. W. TINKER Molecular Mechanics Freeware Package, Version 3.8, October 2000, St. Louis, MO.

(10) Hehre, W. J.; Ditchfield, R.; Pople, J. A. *J. Chem. Phys.* **1972**, *56*, 2257.

(11) Hariharan, P. C.; Pople, J. A. *Theor. Chim. Acta* **1973**, *28*, 213.

(12) Gordon, M. S. *Chem. Phys. Lett.* **1980**, *76*, 163.

(13) McLean, A. D.; Chandler, G. S. *J. Chem. Phys.* **1980**, *72*, 5639.

(14) Krishnan, R.; Binkley, J. S.; Seeger, R.; Pople, J. A. *J. Chem. Phys.* **1980**, *72*, 650.

(15) Sipachev, V. A. *THEOCHEM* **1985**, *22*, 143−51.

(16) Sipachev, V. A. In *Advances in Molecular Structure Research*; Hargittai, I. H., Hargittai, M., Eds.; JAI Press: Greenwich, CT, 1999; Vol. 5, pp 323−371.

(17) Rankin, D. W. H.; Robertson, H. E.; Seip, R.; Schmidbaur, H.; Blaschke, G. *J. Chem. Soc., Dalton Trans.* **1985**, 827.

(18) Hinchley, S. L.; Robertson, H. E.; Borisenko, K. B.; Turner, A. R.; Johnston, B. F.; Rankin, D. W. H.; Ahmadian, M.; Jones, J. N.; Cowley, A. H. *Dalton Trans.* **2004**, 2469.

(19) Ross, A. W.; Fink, M.; Hilderbrandt, R. *International Tables for Crystallography*; Wilson, A. J. C., Ed.; Kluwer Academic Publishers: Dordrecht, Boston, and London, 1992; Vol. C, p 245.